

Adaptive Annotation Distribution for Weakly Supervised Point Cloud Semantic Segmentation

Zhiyi Pan¹, Nan Zhang¹, Wei Gao^{1,✉}, Shan Liu², Ge Li¹

¹School of Electronic and Computer Engineering, Shenzhen Graduate School, Peking University

²Media Laboratory, Tencent

panzhiyi@stu.pku.edu.cn, zhangnan@stu.pku.edu.cn, gaowei262@pku.edu.cn

shanli@tencent.com, geli@ece.pku.edu.cn

Abstract

Weakly supervised point cloud semantic segmentation has attracted a lot of attention due to its ability to alleviate the heavy reliance on fine-grained annotations of point clouds. However, in practice, sparse annotation usually exhibits a distinct non-uniform distribution in point cloud, which poses challenges for weak supervision. To address these issues, we propose an adaptive annotation distribution method for weakly supervised point cloud semantic segmentation. Specifically, we introduce the probability density function into the gradient sampling approximation analysis and investigate the impact of sparse annotations distributions. Based on our analysis, we propose a label-aware point cloud downsampling strategy to increase the proportion of annotations involved in the training stage. Furthermore, we design the multiplicative dynamic entropy as the gradient calibration function to mitigate the gradient bias caused by non-uniformly distributed sparse annotations and explicitly reduce the epistemic uncertainty. Without any prior restrictions and additional information, our proposed method achieves comprehensive performance improvements at multiple label rates with different annotation distributions on S3DIS, ScanNetV2 and SemanticKITTI.

1. Introduction

Point cloud has become one of the most popular 3D representations due to its flexible ability to represent 3D objects and the wide deployment of capture devices. Point cloud semantic segmentation plays a crucial role in various applications [3, 6, 16, 25] by exploiting the abundant 3D geometric information from point clouds. However, point cloud semantic segmentation suffers from heavy reliance on fine-grained annotated point cloud scenes [34]. The increase in data dimensionality brings an order of magnitude increase

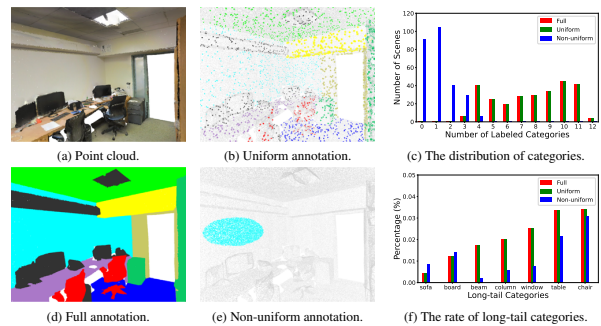


Figure 1. Visual comparison between (b) and (e) at 1% label rate on (a) reveals that uniform annotation is almost unattainable in actual annotation processes. Based on the data presented in (c) regarding the number of labeled categories per scene and in (f) concerning the proportion of long-tail categories, we observe that the distribution disparity between non-uniform sparse annotation and full annotation is more pronounced than that between uniform sparse annotation and full annotation.

in structural complexity and processing difficulty, which further exacerbates the annotation burden. For example, labeling a single point cloud scene in the ScanNetV2 [7] takes an average of 22.3 minutes, while labeling one image in the MS COCO [17] only takes several minutes. Therefore, weakly supervised point cloud semantic segmentation is a promising topic for applications.

Existing methods for weakly supervised point cloud semantic segmentation rely on simulating sparse annotations through uniformly distributed sampling on a fully labeled semantic segmentation dataset. The simulated dataset maintains distribution consistency between sparse and full annotations through uniformly random sampling or "One-Thing-One-Click" [19]. However, this simulated dataset places strict constraints on annotation distribution. In practice, to increase annotation efficiency, annotations are often performed under fewer views, leading to sparse annotation with redundant supervision information. Meanwhile, man-

✉ Corresponding author: Wei Gao.

ual annotators tend to annotate categories that are easier to annotate, exacerbating the long-tail distribution problem. As illustrated in Fig. 1, there is a significant distribution gap between non-uniformly distributed sparse annotations and full annotations, resulting in performance degradation for segmentation models that rely on uniform sampling priors. Therefore, we extend our research to include both non-uniformly and uniformly distributed sparse annotations.

To investigate the impact of non-uniformly distributed annotation on weakly supervised point cloud semantic segmentation, we introduce the probability density function into the gradient sampling approximation analysis [34]. According to the Central Limit Theorem, the gradient discrepancy between weak supervision and full supervision follows a normal distribution, where the distribution type and the proportion of labeling affect its mean and variance, respectively. Based on this analysis, we propose an **Adaptive Annotation Distribution Network (AADNet)** for weakly supervised point cloud semantic segmentation, which is composed of label-aware downsampling strategy and multiplicative dynamic entropy.

Downsampling is essential for point cloud scenes due to computational limitations and data volume. However, random downsampling directly borrowed from the full supervision would miss valuable annotations entailed for training. Conversely, sampling only labeled points would severely sacrifice the structural information from point cloud resampling. Therefore, we propose the label-aware point cloud downsampling strategy (LaDS) to increase the proportion of labeled points involved in the training stage and retain rich structured information to a great extent. To this end, LaDS partitions the point cloud scene into voxel-level and point-level. At the point-level, the labeled points inside each voxel are preferentially sampled, while at the voxel level, the voxels are randomly sampled.

To accommodate various annotation distribution types, we design the multiplicative dynamic entropy with asynchronous training (MDE-AT). We prove that an ideal calibration function for correcting the gradient bias should be inversely proportional to the probability density. However, the probability density of the annotation distribution is agnostic. Therefore, we utilize multiplicative dynamic entropy as an alternative calibration function. Additionally, to improve the epistemic certainty explicitly, we employ asynchronous training that iteratively imposes entropy loss and partial cross-entropy loss with the calibration function.

The effectiveness of our proposed method is evaluated on both uniformly distributed sparse annotation and non-uniformly distributed sparse annotation. Although our method is designed to handle arbitrary non-uniformly distributed sparse annotations, it performs comparably or even outperforms others on S3DIS [1], ScanNetV2 [7] and SemanticKITTI [2] under uniformly distributed sparse anno-

tations, particularly at 0.01% label rates. Extensive ablation studies demonstrate the superiority of our proposed LaDS and MDE-AT. AADNet also shows strong generalizability to various segmentation backbone architectures.

2. Related Work

For weakly supervised point cloud semantic segmentation, researchers have utilized well-established techniques, such as class activation maps [39], perturbation consistency [21], label propagation [12], and contrastive learning [4]. These techniques leverage rich hypothetical priors, processing paradigms, or additional supervision to enable weakly supervised point cloud semantic segmentation. Rather than relying on a single technique, most methods build their effective weak supervision frameworks by integrating multiple techniques.

Class Activation Maps. Class Activation Maps (CAMs) has been widely used in image-level weakly supervised semantic segmentation tasks due to its semantic localization capability. Similarly, in weakly supervised point cloud semantic segmentation, CAMs have been used to provide category localization information for both scene-level and sub-scene-level annotations. To further improve the semantic localization capability of CAMs, MPRM [30] proposes a multi-path region mining module to mine various region information. Song *et al.*[28] act CAMs and geometric projection to obtain point-level pseudo-label. MILTrans [35] utilizes an adaptive global weighted pooling mechanism on CAMs to mitigate the negative effects of irrelevant classes and noisy points.

Perturbation Consistency. A replica of the original point cloud can be generated by perturbing. Consistency between the corresponding features of the original and replica point clouds can be exploited to provide additional supervision under sparse annotation. To this end, Xu *et al.* [34] applies perturbations such as rotation and mirror flipping to the point cloud scene, while PSD [38] exploits the rotation of the point cloud and the jitter of the points with attribute attention layers. MILTrans [35] maintains feature consistency on the pair point clouds before and after downsampling. DAT [32] and HybridCR [15] dynamically construct point cloud replicas using adaptive gradient and embedding network learning, respectively. Recently, RPSC [13] and PointMatch [31] leverage pseudo-labels to convey consistent information.

Label Propagation. The label propagation algorithm is a common technique for generating high-quality pseudo-labels in self-training. OTOC [19] and OTOC++ [20] propose RelationNets to accurately measure the similarity between 3D graph nodes and propagate labeling information. Zhang *et al.* [37] develops a sparse label propagation algorithm guided by the category prototype [27], where a category assignment matrix is constructed based on the similar-

ity between the category prototype and the feature embedding. SSPC-Net [5] is based on the super point-level graph topology for label propagation and introduces a coupled attention mechanism to learn contextual features between labeled and pseudo-labeled super-points.

Contrastive learning. Contrastive learning selects anchor points in point clouds, and then strategically imposes restrictions on corresponding positive point pairs and negative point pairs. HybridCR [15] constructs contrastive learning on transformed point cloud pairs, local geometry pairs, and category prototypes pairs, while MILTrans [35] utilizes cross attention transformer on point clouds to achieve multiple instance learning and perform contrastive loss between category pairs in the scene. Besides, pre-training methods such as PointContrast [33] and Hou *et al.* [9], utilize contrastive learning without any label. With high generality for downstream tasks, these pre-trained models can also achieve semantic segmentation tasks using few annotations.

Others. SQN [11] takes any location in the scene as input and then collects a group of hierarchical representations within the locally labeled neighborhoods through interpolation. Based on these representations, SQN predicts the category of the queried location. GaIA [14] proposes the Entropy Block to actively reduce the graphical information gain and the anchor-based additive angular margin loss to optimize the uncertain points.

The above methods are verified under the uniformly distributed sparse annotations. However, uniformly distributed sampling is elusive to achieve for manual annotators. Consequently, we propose a point cloud semantic segmentation method with adaptive annotation distribution for arbitrary sparse annotation scenarios.

3. Method

We give a brief overview of weakly supervised point cloud semantic segmentation in Sec. 3.1. Then the probability density function is introduced into the gradient sampling approximation analysis to investigate the non-uniform distribution annotation in Sec. 3.2. Based on the analysis, we propose the Adaptive Annotation Distribution Network, which is composed of label-aware downsampling strategy (Sec. 3.3) and multiplicative dynamic entropy (Sec. 3.4). The framework of AADNet is illustrated in Fig. 2.

3.1. Overview

A point cloud scene in the train set for semantic segmentation can be denoted as $\mathbf{P} = \{\mathbf{X}, \mathbf{Y}\}$, where \mathbf{X} and \mathbf{Y} represent point set and its corresponding label, respectively. In detail, $\mathbf{X} = [\mathbf{x}_1, \mathbf{x}_2, \dots, \mathbf{x}_N]$ and $\mathbf{x}_i \in \mathbb{R}^F$, in which N denotes the number of points and F is the dimension number of initial feature on each point \mathbf{x}_i . Without losing generality, $\mathbf{Y} = [\mathbf{y}_1, \mathbf{y}_2, \dots, \mathbf{y}_M]$ and $\mathbf{y}_i \in \{0, 1\}^C$, where M and C indicate the number of labeled points and categories,

respectively. When $N \gg M$, the task is termed as a weakly supervised point cloud semantic segmentation task, and the label rate is $\frac{M}{N}$. The partial cross-entropy loss, which is commonly used in weak supervision, is defined as:

$$\mathcal{L}_p = \frac{1}{M} \sum_{i=1}^M \ell(\mathbf{y}_i, \hat{\mathbf{y}}_i) = \frac{1}{M} \sum_{i=1}^M \sum_{c=1}^C y_{ic} \log(\hat{y}_{ic}), \quad (1)$$

where $\hat{\mathbf{y}}_i \in [0, 1]^C$ denotes the prediction probability at \mathbf{x}_i .

3.2. Gradient Sampling Approximation Analysis

For two networks with the same structure and initialization parameters, it is assumed that the closer the gradients are, the more likely they will converge to the same prediction results for the same input. The gradients of cross-entropy $\nabla \mathcal{L}$ and partial cross-entropy $\nabla \mathcal{L}_p$ are formulated as:

$$\begin{aligned} \nabla \mathcal{L} &= \frac{1}{N} \sum_{i=1}^N g(\hat{\mathbf{y}}_i), \\ \nabla \mathcal{L}_p &= \frac{1}{M} \sum_{i=1}^M g(\hat{\mathbf{y}}_i), \end{aligned} \quad (2)$$

where $g(\hat{\mathbf{y}}_i) = \nabla \ell(\mathbf{y}_i, \hat{\mathbf{y}}_i)$, denotes the loss gradient at \mathbf{x}_i . Weakly supervised learning can be viewed as fully supervised learning with M times sampling of gradients, and the average gradient value of M times sampling is equal to $\nabla \mathcal{L}_p$. Assuming that $g(\hat{\mathbf{y}}_i)$ satisfies the independent identical distribution, the uniformly distributed sampled $s(g(\hat{\mathbf{y}}_i))$ follows the distribution $\mathcal{D}_u(E_u, V_u)$. The expectation $E_u = \mathbb{E}_{\mathbf{x}_i \sim \mathcal{D}}[p_i g(\hat{\mathbf{y}}_i)] = \sum_i \frac{1}{N} g(\hat{\mathbf{y}}_i) = \nabla \mathcal{L}$, where \mathcal{D} is the distribution of points and $p_i = \frac{1}{N}$ denotes the probability density function of uniformly distributed sampling. According to the Central Limit Theorem, the following convergent distribution can be obtained under uniformly distributed sampling (see Supplementary Materials for details):

$$(\nabla \mathcal{L}_p - \nabla \mathcal{L}) \sim \mathcal{N}(0, \frac{V_u}{M}). \quad (3)$$

Eq. 3 illustrates that the gradient difference between full annotations and uniformly sparse annotations obeys a normal distribution with 0 expectation and $\frac{V_u}{M}$ variance. Eq. 3 indicates that the average gradient of uniform sparse annotations is more likely to be similar to that of full annotations when the label rate becomes larger.

Based on the previous assumption, the prediction results of the model supervised by uniform sparse annotations at an appropriate label rate are consistent with those of the fully supervised semantic segmentation model. However, this corollary is not universal for the non-uniformly distributed sparse annotations. We assume that non-uniformly sampled gradient $s_n(g(\hat{\mathbf{y}}_i))$ follows the distribution $\mathcal{D}_n(E_n, V_n)$. The expectation $E_n = \mathbb{E}_{\mathbf{x}_i \sim \mathcal{D}}[p'_i g(\hat{\mathbf{y}}_i)] = \sum_i p'_i g(\hat{\mathbf{y}}_i) =$

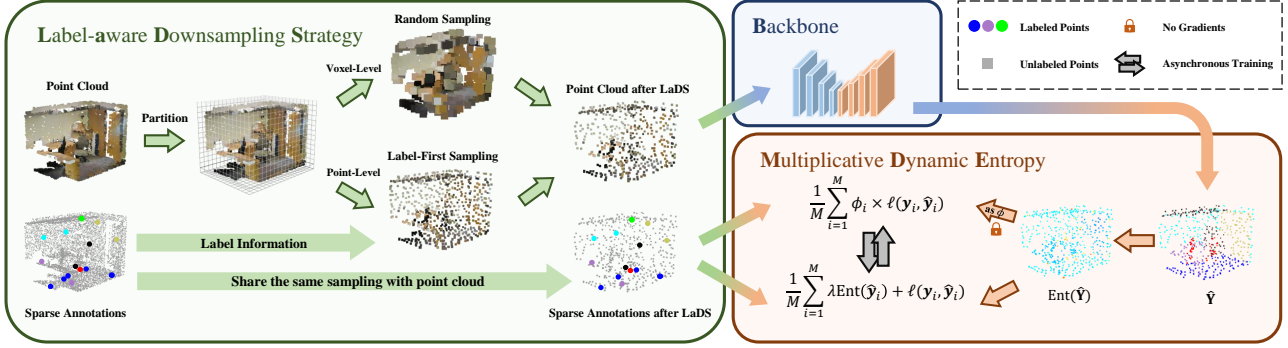


Figure 2. The framework of AADNet consists of two parts: (1) Label-aware downsampling strategy (LaDS) to boost the training annotation rate and maintain structural diversity. (2) Multiplicative dynamic entropy with asynchronous training (MDE-AT) to correct for gradient bias due to sparse labeling distributions as well as to explicitly improve the epistemic certainty.

$\nabla \mathcal{L} + \Delta$, where p'_i denotes the probability density function of the non-uniformly sampling distribution and the bias $\Delta = \sum_i (p'_i - p_i) g(\hat{y}_i)$. Similarly, according to the Central Limit Theorem, we obtain the following convergent distribution under non-uniformly distributed sampling:

$$(\nabla \mathcal{L}_p - \nabla \mathcal{L}) \sim \mathcal{N}(\Delta, \frac{V_n}{M}). \quad (4)$$

Eq. 4 demonstrates that in the case of non-uniformly distributed sparse annotations, the average gradient still differs by Δ even at large label rates. Therefore, the performance of weak supervision is not only related to the label rate, but also to the annotation distribution type. Without other priors, uniformly distributed sparse labeling is the optimal sparse labeling.

3.3. Label-aware Downsampling Strategy

The downsampling strategy plays a crucial role in subsequent network training because it determines the upper bound of the receptive field and the diversity of the structural information of the scene [10]. However, the random downsampling strategy used by full supervision is not applicable to sparse labeling scenarios, for which the random downsampling treats labeled and unlabeled points equally, it will significantly weaken the semantic supervision information of the sampled point cloud. An intuitive alternative is preferentially selecting all labeled points. Although it can greatly preserve labeled points after downsampling, it compromises the diversity of structural information when sampling the point cloud repeatedly. Therefore, a label-aware downsampling strategy is proposed to preserve both labeled points and abundant structural topology.

The label-aware point cloud downsampling strategy is shown in Fig. 2. First, we partition the entire point cloud scene by voxels, and then decompose the downsampling into point-level downsampling and voxel-level downsampling. At the point-level, for the voxel that contains labeled

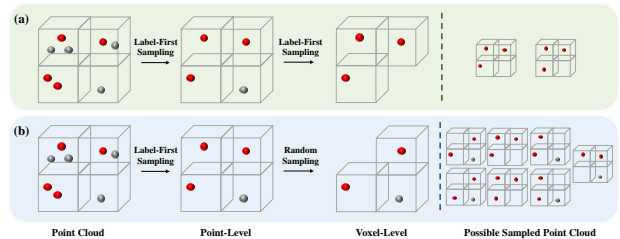


Figure 3. Compared with (a) with voxel-level label-first downsampling, (b) with voxel-level random downsampling retains diverse scene structural information.

points, one labeled point is randomly selected among the labeled points within the voxel, and for the voxel that does not contain any labeled point, one point is randomly selected within the voxel. Although there is a risk of loss of structural diversity with point-level label-first sampling, it is almost negligible because the sampling is over a small range of a voxel, and point jitter in subsequent data augmentation is able to compensate for this topological loss. While at the voxel-level, we retain the conventional random downsampling strategy. In contrast to voxel-level label-first downsampling, voxel-level random downsampling sacrifices a small percentage of the label rate, but acquires diverse scene structural information when sampling repeatedly in different training epochs. Sampling strategies with voxel-level label-first downsampling and voxel-level random downsampling are visualized in Fig. 3 for comparison.

Overall, LaDS is an annotation distribution-independent sampling strategy and retains annotation indiscriminately for arbitrary sparse annotation distributions. Simple but effective, LaDS is able to improve the training label rate by 2 to even 10 times at 0.01% label rate of the dataset.

3.4. Multiplicative Dynamic Entropy

Based on the methodological analysis in Section 3.2, we propose to impose a gradient calibration function ϕ on \mathcal{L}_p to counteract the impact on the gradient expectation caused by the non-uniformly distributed sparse annotations. Ideally, using multiplicative calibration function $\phi_i = \frac{p'_i}{p_i}$, the expectation of the corrected gradient satisfies:

$$E_n = \mathbb{E}_{\mathbf{x}_i \sim \mathcal{D}}[p'_i \phi_i g(\hat{\mathbf{y}}_i)] = \mathbb{E}_{\mathbf{x}_i \sim \mathcal{D}}[p_i g(\hat{\mathbf{y}}_i)] = \nabla \mathcal{L}. \quad (5)$$

The gradient bias Δ is correct by ϕ . Compared to the ideal additive calibration function $\psi_i = (p'_i - p_i)g(\hat{\mathbf{y}}_i)$, the multiplicative calibration function ϕ is gradient-independent and easier to estimate.

Nevertheless, the probability density function p'_i of non-uniformly distributed sampling in the ideal ϕ is agnostic. Due to the correlation with annotators and the point cloud dataset, we choose the multiplicative calibration function cautiously based on the following two criteria: (1) Since the fixed weights as ϕ cannot adaptively correct for different point cloud scenes, ϕ should be a dynamic function related to sparsely labeled scenes in the training stage. (2) The classification difficulty of points reflects the annotation difficulty. Therefore, taking the negative correlation between labeling difficulty and labeling probability p'_i as a guideline, we utilize the entropy function as the dynamic calibration function, *i.e.*, $\phi_i = \text{Ent}(\hat{\mathbf{y}}_i) = \sum_c \hat{\mathbf{y}}_{ic} \log(\hat{\mathbf{y}}_{ic})$, where c denotes the category index. It is worth noting that although ϕ is a function on predictions $\hat{\mathbf{Y}}$, it does not generate gradients during training, but only serves to weight the partial cross-entropy loss dynamically.

In order to make entropy more accurately reflect the difficulty of point classification and reduce the epistemic uncertainty of the network under weak supervision, we further use entropy as a loss term. However, if the entropy function is allowed to backpropagation gradients in a simultaneous way to reduce the epistemic uncertainty, it will change the optimization objective of the network and make the partial cross-entropy loss not converge. Therefore, we utilize asynchronous training to explicitly reduce the epistemic uncertainty. The total loss function $\mathcal{L}_{\text{AAD}}^k$ at the k -th training epoch is defined as:

$$\begin{aligned} \mathcal{L}_{\text{AAD}}^k &= \mathbb{1}(k \bmod 2\tau \geq \tau) \frac{1}{M} \sum_{i=1}^M \left[\phi_i \times \ell(\mathbf{y}_i, \hat{\mathbf{y}}_i) \right] + \\ &\quad \mathbb{1}(k \bmod 2\tau < \tau) \frac{1}{M} \sum_{i=1}^M \left[\lambda \text{Ent}(\hat{\mathbf{y}}_i) + \ell(\mathbf{y}_i, \hat{\mathbf{y}}_i) \right], \end{aligned} \quad (6)$$

where $\mathbb{1}(\cdot)$ denotes the indicator function, λ is a predefined balance weight, and τ denotes the step interval of asynchronous training. To learn efficiently, AADNet still imposes partial cross-entropy loss while learning on $\text{Ent}(\hat{\mathbf{y}}_i)$.

4. Experiments

We evaluate our AADNet on S3DIS [1], ScanNetV2 [7] and SemanticKITTI [2] with both uniformly and non-uniformly distributed sparse annotations. The mean Intersection over Union (mIoU) is adopted as the evaluation metric.

4.1. Experiment Setting

Dataset. S3DIS [1] contains 271 rooms in six areas, covering over 6,000 square meters. In total, the dataset has over 2.15 million points with 13 semantic categories. We train our model on Area 1, 2, 3, 4 and 6, and evaluate the segmentation performance on Area 5. ScanNetV2 [7] consists of 1,513 scanned scenes obtained from 707 different indoor environments and provides 21 semantic categories for each point. We utilize 1,201 scenes for training and 312 scenes for validation, as per the official split. In addition to the two indoor point cloud datasets, the outdoor dataset SemanticKITTI [2] with 19 classes is also considered. Point cloud sequences 00 to 10 are used in training, with sequence 08 as the validation set.

Sparse label. Our method is validated under sparse annotations with both uniform distribution and non-uniform distribution, respectively. Uniformly distributed sampling is used to simulate sparse annotations by proportional random downsampling [34] or one-thing-one-click [19], and we adopt the proportional random downsampling due to its less restrictive to the annotation process. In the uniform sparse annotations setting, we report weakly supervised segmentation performance at 0.1%, and 0.01% on S3DIS and SemanticKITTI, and 1% and 20 points per scene (label rate is about 0.014%) on ScanNetV2. For simulating the non-uniform label, we randomly sample a point in the scene as the center point, and then calculate the color space and Euclidean space distances between the points in the scene and the center point. Then the nearest neighbors are selected proportionally (10% or 1%) to generate non-uniformly distributed sparse annotations. An example of non-uniform annotations is shown in Fig. 1e. Segmentation benchmarks under non-uniform sparse annotations at 10% and 1% label rates are provided.

Implementation. We choose PointNeXt-L [24] as the backbone for indoor datasets and SparseConv [8] for outdoor dataset SemanticKITTI. We use the default settings to construct our weakly supervised point cloud segmentation framework. To prevent the entropy loss from misleading the network during the early stage of training [21], we set the start epoch of asynchronous training to 50. The weight $\lambda = 0.01$ and step interval $\tau = 5$ in Eq. 6. Our models are trained with one NVIDIA V100 GPU on S3DIS, eight NVIDIA TESLA T4 GPUs on ScanNetV2, and four NVIDIA V100 GPUs on SemanticKITTI.

Method	S3DIS Area 5				ScanNetV2 Test				SemanticKITTI Val.			
	$\geq 0.1\%$		$\sim 0.01\%$		$\sim 1\%$		$\sim 0.01\%$		$\geq 0.1\%$		$\sim 0.01\%$	
	Rate	mIoU	Rate	mIoU	Rate	mIoU	Rate	mIoU	Rate	mIoU	Rate	mIoU
Zhang <i>et al.</i> [37]	1%	61.8	0.03%	45.8	1%	51.1	-	-	-	-	-	-
PSD [38]	1%	63.5	0.03%	48.2	1%	54.7	-	-	-	-	-	-
HybirdCR [†] [15]	1%	65.3	0.03%	51.5	1%	56.8	-	-	1%	51.9	-	-
GaIA [14]	1%	66.5	0.02%	53.7	1%	65.2	20 pts	63.8	-	-	-	-
DCL [†] [36]	1%	67.2	0.02%	58.2	1%	59.6	-	-	1%	52.6	-	-
RPSC [13]	0.1%	63.1	0.04%	64.0	-	-	50 pts	58.7	0.1%	50.9	-	-
OTOC [†] [19]	-	-	0.02%	50.1	-	-	20 pts	59.4	-	-	-	-
MILTrans [35]	-	-	0.02%	51.4	-	-	20 pts	54.4	-	-	-	-
DAT [32]	-	-	0.02%	56.5	-	-	20 pts	55.2	-	-	-	-
OTOC++ [†] [20]	-	-	0.02%	56.6	-	-	0.01%	60.6	-	-	-	-
CPCM [18]	0.1%	66.3	0.01%	59.3	-	-	0.01%	52.2	0.1%	44.0	0.01%	34.7
SQN [11]	0.1%	61.4	0.01%	45.3	-	-	-	-	0.1%	50.8	0.01%	39.1
PointMatch [†] [31]	0.1%	63.4	0.01%	59.9	-	-	20 pts	62.4	-	-	-	-
AADNet (improvement)	0.1%	67.2 ($\uparrow 2.9$)	0.01%	60.8 ($\uparrow 16.1$)	1%	66.8 ($\uparrow 3.2$)	20 pts	62.5 ($\uparrow 11.0$)	0.1%	61.8 ($\uparrow 5.9$)	0.01%	50.8 ($\uparrow 6.6$)

Table 1. Quantitative comparison on weakly supervised point cloud semantic segmentation methods under uniform sparse annotations. 0.02% on S3DIS denotes the one-thing-one-click annotation. 20 pts on Scannetv2 denotes 20 points per scene annotation. [†] indicates that pseudo-labels are used during the network training stage.

Method	S3DIS Area 5		ScanNetV2 Val.	
	10%	1%	10%	1%
DCL [†] [36]	52.9	35.6	55.1	34.7
CPCM [18]	54.9	38.2	59.5	41.7
Baseline	54.1	35.9	56.0	37.0
AADNet	56.0	39.0	61.2	43.4

Table 2. Quantitative comparisons under non-uniform annotations. [†] indicates that pseudo-label is used.

4.2. Comparison Results

In Tab. 1, we conduct a comprehensive comparison of three datasets with various uniformly distributed sparse annotations. Unlike other methods, our approach does not rely on additional annotation restrictions and over-segmentation information to expand the original sparse label. However, AADNet still outperforms other alternative methods designed for uniform distribution sparse annotations in all weakly supervised settings. For S3DIS [1], the segmentation performance of our method at 0.1% uniform label rate is even comparable to that of fully supervised KPConv [29]. In particular, with $10,000\times$ fewer annotations, our method achieves 88.1% segmentation performance of full supervision. For ScanNetV2 [7], AADNet achieves a comparable mIoU to PointMatch [31] on 20 points per scene annotation setting, but without the aid of pseudo-labeling. To demon-

strate the generalizability of AADNet, we also report the semantic segmentation performance on the outdoor dataset SemanticKITTI [2]. As shown in Tab. 1, AADNet brings 5.9% and 6.6% mIoU improvements to the baseline at 0.1% and 0.01% label rates, respectively. Overall, the improvement delivered by AADNet is more significant at extreme label rate, due to the ability of AADNet to explicitly increase the number of annotations involved in training and to mitigate the non-uniformly distributed annotations presented by extreme limited label rate.

For better comparison, we reproduce two recently published and open-sourced methods [18, 36] in our non-uniform distribution sparse labeling scenario. Tab. 2 illustrates that non-uniform annotation poses a significant hindrance to network learning. Even at a 10% label rate, the segmentation performance under non-uniformly distributed annotation is worse than that under 0.1% uniformly distributed annotation. Nevertheless, our method still improves the mIoU by 1.9% and 3.1% on S3DIS, 5.2% and 6.4% on ScanNetV2 compared to the baseline at 10% and 1% label rates, respectively, which demonstrate the effectiveness of AADNet under various distribution annotations.

In addition, we present a qualitative comparison of the method with the baseline in Fig. 4. Due to the lack of sufficient supervisory information, the baseline has a significant performance degradation on categories with variable forms, such as bookcase with miscellaneous books and clutter on tables, and categories that are easily confused, such as wall, column, and board. Conversely, AADNet shows more com-

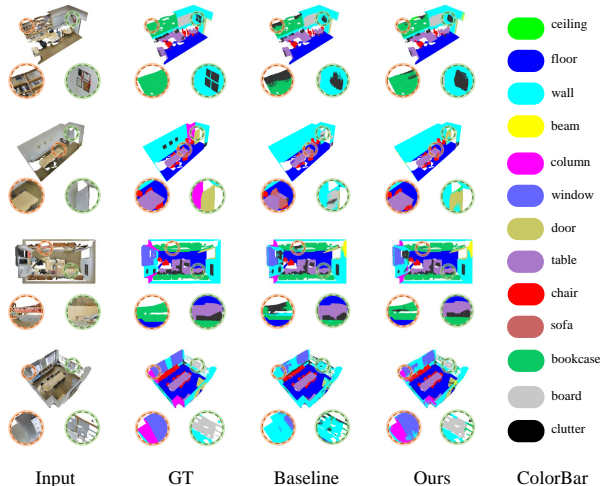


Figure 4. Qualitative comparisons on S3DIS under various label settings. From top to bottom, the label settings are 10% non-uniform, 1% non-uniform, 0.1% uniform, and 0.01% uniform sparse annotations. Significant differences are highlighted in order to observe the enhancement. Zoom-in for better visualization.

plete predictions for head categories and more accurate predictions for long-tail categories compared to the baseline.

4.3. Ablation Study

We perform extensive ablation experiments for the proposed method on S3DIS Area 5 to verify the effectiveness of each module. We also report the ablation results of our method on various annotation distributions to demonstrate the robustness of our method under different sparse labeling environments. Baseline denotes the point cloud semantic segmentation network PointNeXt-L [24] trained with the official default settings.

Label-first Sampling		Uniform		Non-uniform	
Point	Voxel	0.01%	0.1%	1%	10%
	✓	44.7	64.3	35.9	54.1
✓	✓	45.6	65.0	36.4	54.0
✓	✓	58.1	66.6	37.0	53.8
✓	✓	58.4	67.0	37.8	54.8

Table 3. Ablation study for LaDS on S3DIS Area 5.

Ablation on LaDS. Tab. 3 demonstrates the segmentation performance with or without the label-first sampling. It can be observed that both point-level label-first downsampling and voxel-level label-first downsampling promote the segmentation performance. However, voxel-level label-first downsampling may destroy the sampling diversity of resampling and therefore ignores part of the geometric topol-

ogy. Hence, using both voxel-level and point-level label-first downsampling is suboptimal. The optimal performance is achieved by only using point-level label-first sampling (*i.e.*, LaDS), which improves the label rate while avoiding compromising sampling diversity.

Setting	Uniform		Non-uniform	
	0.01%	0.1%	1%	10%
Baseline	44.7	64.3	35.9	54.1
+ FixedW	43.3	60.5	35.6	55.1
+ ADE	48.2	64.7	36.3	55.0
+ MDE-ST	-	-	-	-
+ MDE-AT	49.7	65.0	36.8	56.0

Table 4. Ablation study for MDE-AT on S3DIS Area 5. '-' indicates that partial cross-entropy loss does not converge.

Ablation on MDE-AT. We validate several feasible gradient calibration functions in Tab. 4. FixedW sets the inverse of the local density of points as the gradient calibration function, and the value of FixedW is fixed during training. ADE denotes the Additive Dynamic Entropy. MDE-ST and MDE-AT denote the multiplicative dynamic entropy with simultaneous training and asynchronous training, respectively. By observing the metrics under different annotation settings, we have the following inferences: Fixed weights cannot adjust the weights dynamically for different point clouds. The additive calibration function is difficult to learn compared with the multiplicative calibration function. Simultaneous training changes the learning objective of the partial cross-entropy loss function, leading to the partial cross-entropy loss function failing to converge. However, our proposed MDE-AT is not only able to handle non-uniformly distributed annotation environments adaptively, but also has the ability to cope with distribution differences between full annotation and uniformly distributed sparse annotation.

τ	Uniform		Non-uniform	
	0.01%	0.1%	1%	10%
1	48.6	65.1	36.1	55.7
5	49.7	65.0	36.8	56.0
10	49.5	65.4	36.8	55.1
25	48.8	64.7	36.6	55.5
50	48.8	65.1	36.3	54.8

Table 5. Performance comparison with different step intervals on S3DIS Area 5.

Step interval parameter search. We search the step inter-

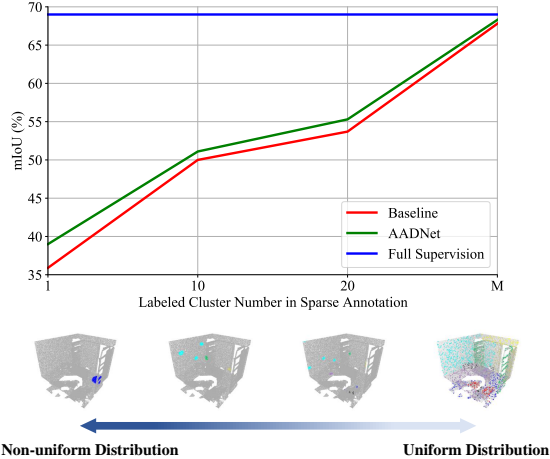


Figure 5. Comparisons between Baseline and AADNet on various non-uniform annotation forms on S3DIS Area 5.

val τ for MDE-AT in Tab. 5. The results indicate a trend of increasing performance with increasing τ , followed by a subsequent decrease. A small τ may cause the network learning difficulty and converging adequately. Conversely, a large τ may bias the network to give overconfident predictions, thus making the prediction results noisy. The overall performance is insensitive to the τ . Based on the experimental results, we set the step interval as 5.

4.4. Further Analysis

More non-uniform annotation forms. We extend the non-uniformly distributed sparse annotation experimental setup from single labeled cluster to multiple labeled clusters. At the same label rate, when the number of labeled clusters increases, the number of points inside the corresponding clusters decreases. In particular, when the number of labeled clusters coincides with the number of labeled points M , the annotation distribution degrades to a uniform distribution. Fig. 5 shows the performance of different non-uniform annotation forms at the 1% label rate, which indicates that our proposed AADNet has a wide range of performance improvement over the baseline on various non-uniform sparse annotation forms.

Robustness study with different backbones. The backbone has a direct impact on the performance of weakly supervised segmentation. However, existing weakly supervised methods employ different backbone networks, making it difficult to align backbones for comparison. To rule out the effect of backbone, we report the segmentation performance improvements of AADNet with different backbones. In addition to using three common point cloud segmentation backbones [22–24], we are also using weakly supervised method DCL [36] directly as the back-

Method	Backbone	Full 100%	Uniform		Non-uniform	
			0.01%	0.1%	1%	10%
Baseline	PointNet++ [22]	63.4	47.8	60.0	34.3	50.3
Ours	PointNet++ [22]	63.4	53.3	60.0	36.6	50.8
Baseline	ASSANet [23]	66.1	40.4	62.4	37.7	52.8
Ours	ASSANet [23]	66.0	60.7	64.4	38.9	54.1
Baseline	DCL [36]	67.8	39.8	60.7	35.6	52.9
Ours	DCL [36]	67.9	54.0	67.2	38.0	55.7
Baseline	PointNeXt [24]	69.0	44.7	64.3	35.9	54.1
Ours	PointNeXt [24]	69.2	60.8	67.2	39.0	56.0

Table 6. Robustness study with different backbones on S3DIS Area 5.

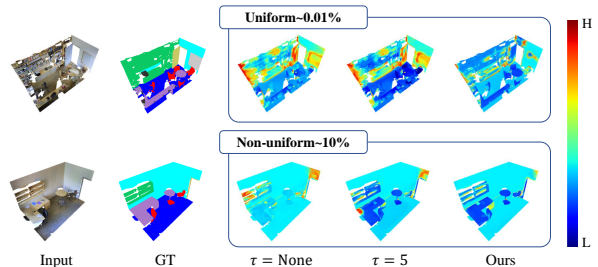


Figure 6. The input point cloud (Input), ground truth (GT), and corresponding entropy on MDE without asynchronous training (τ is None), MDE-AT ($\tau = 5$) and AADNet (Ours).

bone. In Tab. 6, the enhancements from AADNet are consistent across different backbones. In particular, with the weakly supervised method DCL as the backbone, AADNet still obtains a 14.2% mIoU improvement at 0.01% label rate. Therefore, AADNet is not only adaptive to sparse annotation distributions but also inclusive to backbones.

Epistemic uncertainty. Shannon entropy [26] can be used as a measure of the epistemic uncertainty of the network [14]. Fig. 6 visualize the entropy of predicted class probability. High-entropy areas are located in objects with variable forms and objects that are easily confused. By explicitly learning the entropy of the labeled points with asynchronous training, the entropy of these objects is significantly reduced, resulting in a reliable and robust semantic segmentation network. Finally, AADNet has less epistemic uncertainty by combining LaDS and MDE-AT.

5. Conclusion

In this paper, we provide benchmarks for semantic segmentation on S3DIS, ScanNetV2, and SemanticKITTI with various distribution sparse annotations. By introducing the probability density function into the gradient sampling approximation analysis, we reveal the impact of sparse annotation distributions in the manual labeling process. Based

on gradient analysis, we propose an adaptive annotation distribution network, consisting of the label-aware down-sampling strategy and the multiplicative dynamic entropy for asynchronous training. Without any prior restrictions and additional information, AADNet achieves comprehensive performance improvements with different annotation distributions. We expect that our work can provide novel research insights for the weakly supervised point cloud semantic segmentation community.

References

- [1] Iro Armeni, Ozan Sener, Amir R Zamir, Helen Jiang, Ioannis Brilakis, Martin Fischer, and Silvio Savarese. 3d semantic parsing of large-scale indoor spaces. In *Proceedings of the IEEE conference on computer vision and pattern recognition*, pages 1534–1543, 2016. 2, 5, 6
- [2] Jens Behley, Martin Garbade, Andres Milioto, Jan Quenzel, Sven Behnke, Cyrill Stachniss, and Jurgen Gall. Semantickitti: A dataset for semantic scene understanding of lidar sequences. In *Proceedings of the IEEE/CVF international conference on computer vision*, pages 9297–9307, 2019. 2, 5, 6
- [3] Thomas Blanc, Mohamed El Beheiry, Clément Caporal, Jean-Baptiste Masson, and Bassam Hajj. Genuage: visualize and analyze multidimensional single-molecule point cloud data in virtual reality. *Nature Methods*, 17(11):1100–1102, 2020. 1
- [4] Ting Chen, Simon Kornblith, Mohammad Norouzi, and Geoffrey Hinton. A simple framework for contrastive learning of visual representations. In *International conference on machine learning*, pages 1597–1607. PMLR, 2020. 2
- [5] Mingmei Cheng, Le Hui, Jin Xie, and Jian Yang. Sspc-net: Semi-supervised semantic 3d point cloud segmentation network. In *Proceedings of the AAAI conference on artificial intelligence*, pages 1140–1147, 2021. 3
- [6] Yaodong Cui, Ren Chen, Wenbo Chu, Long Chen, Daxin Tian, Ying Li, and Dongpu Cao. Deep learning for image and point cloud fusion in autonomous driving: A review. *IEEE Transactions on Intelligent Transportation Systems*, 23(2): 722–739, 2021. 1
- [7] Angela Dai, Angel X Chang, Manolis Savva, Maciej Halber, Thomas Funkhouser, and Matthias Nießner. Scannet: Richly-annotated 3d reconstructions of indoor scenes. In *Proceedings of the IEEE conference on computer vision and pattern recognition*, pages 5828–5839, 2017. 1, 2, 5, 6
- [8] Benjamin Graham, Martin Engelcke, and Laurens Van Der Maaten. 3d semantic segmentation with submanifold sparse convolutional networks. In *Proceedings of the IEEE conference on computer vision and pattern recognition*, pages 9224–9232, 2018. 5
- [9] Ji Hou, Benjamin Graham, Matthias Nießner, and Saining Xie. Exploring data-efficient 3d scene understanding with contrastive scene contexts. In *Proceedings of the IEEE/CVF Conference on Computer Vision and Pattern Recognition*, pages 15587–15597, 2021. 3
- [10] Qingyong Hu, Bo Yang, Linhai Xie, Stefano Rosa, Yulan Guo, Zhihua Wang, Niki Trigoni, and Andrew Markham. Randla-net: Efficient semantic segmentation of large-scale point clouds. In *Proceedings of the IEEE/CVF conference on computer vision and pattern recognition*, pages 11108–11117, 2020. 4
- [11] Qingyong Hu, Bo Yang, Guangchi Fang, Yulan Guo, Aleš Leonardis, Niki Trigoni, and Andrew Markham. Sqn: Weakly-supervised semantic segmentation of large-scale 3d point clouds. In *Computer Vision—ECCV 2022: 17th European Conference, Tel Aviv, Israel, October 23–27, 2022, Proceedings, Part XXVII*, pages 600–619. Springer, 2022. 3, 6
- [12] Ahmet Iscen, Giorgos Tolias, Yannis Avrithis, and Ondrej Chum. Label propagation for deep semi-supervised learning. In *Proceedings of the IEEE/CVF conference on computer vision and pattern recognition*, pages 5070–5079, 2019. 2
- [13] Yuxiang Lan, Yachao Zhang, Yanyun Qu, Cong Wang, Chengyang Li, Jia Cai, Yuan Xie, and Zongze Wu. Weakly supervised 3d segmentation via receptive-driven pseudo label consistency and structural consistency. In *Proceedings of the AAAI Conference on Artificial Intelligence*, pages 1222–1230, 2023. 2, 6
- [14] Min Seok Lee, Seok Woo Yang, and Sung Won Han. Gaia: Graphical information gain based attention network for weakly supervised point cloud semantic segmentation. In *Proceedings of the IEEE/CVF Winter Conference on Applications of Computer Vision*, pages 582–591, 2023. 3, 6, 8
- [15] Mengtian Li, Yuan Xie, Yunhang Shen, Bo Ke, Ruizhi Qiao, Bo Ren, Shaohui Lin, and Lizhuang Ma. Hybridcr: Weakly-supervised 3d point cloud semantic segmentation via hybrid contrastive regularization. In *Proceedings of the IEEE/CVF Conference on Computer Vision and Pattern Recognition*, pages 14930–14939, 2022. 2, 3, 6
- [16] Ying Li, Lingfei Ma, Zilong Zhong, Fei Liu, Michael A Chapman, Dongpu Cao, and Jonathan Li. Deep learning for lidar point clouds in autonomous driving: A review. *IEEE Transactions on Neural Networks and Learning Systems*, 32(8):3412–3432, 2020. 1
- [17] Tsung-Yi Lin, Michael Maire, Serge Belongie, James Hays, Pietro Perona, Deva Ramanan, Piotr Dollár, and C Lawrence Zitnick. Microsoft coco: Common objects in context. In *Computer Vision—ECCV 2014: 13th European Conference, Zurich, Switzerland, September 6–12, 2014, Proceedings, Part V 13*, pages 740–755. Springer, 2014. 1
- [18] Lizhao Liu, Zhuangwei Zhuang, Shangxin Huang, Xunlong Xiao, Tianhang Xiang, Cen Chen, Jingdong Wang, and Mingkui Tan. Cpcm: Contextual point cloud modeling for weakly-supervised point cloud semantic segmentation. In *Proceedings of the IEEE/CVF International Conference on Computer Vision*, pages 18413–18422, 2023. 6
- [19] Zhengzhe Liu, Xiaojuan Qi, and Chi-Wing Fu. One thing one click: A self-training approach for weakly supervised 3d semantic segmentation. In *Proceedings of the IEEE/CVF Conference on Computer Vision and Pattern Recognition*, pages 1726–1736, 2021. 1, 2, 5, 6
- [20] Zhengzhe Liu, Xiaojuan Qi, and Chi-Wing Fu. One thing one click++: Self-training for weakly supervised 3d scene understanding. *arXiv preprint arXiv:2303.14727*, 2023. 2, 6

- [21] Zhiyi Pan, Peng Jiang, Yunhai Wang, Changhe Tu, and Anthony G Cohn. Scribble-supervised semantic segmentation by uncertainty reduction on neural representation and self-supervision on neural eigenspace. In *Proceedings of the IEEE/CVF International Conference on Computer Vision*, pages 7416–7425, 2021. 2, 5
- [22] Charles Ruizhongtai Qi, Li Yi, Hao Su, and Leonidas J Guibas. Pointnet++: Deep hierarchical feature learning on point sets in a metric space. *Advances in neural information processing systems*, 30, 2017. 8
- [23] Guocheng Qian, Hasan Hammoud, Guohao Li, Ali Thabet, and Bernard Ghanem. Assanet: An anisotropic separable set abstraction for efficient point cloud representation learning. *Advances in Neural Information Processing Systems*, 34:28119–28130, 2021. 8
- [24] Guocheng Qian, Yuchen Li, Houwen Peng, Jinjie Mai, Hasan Hammoud, Mohamed Elhoseiny, and Bernard Ghanem. Pointnext: Revisiting pointnet++ with improved training and scaling strategies. *Advances in Neural Information Processing Systems*, 35:23192–23204, 2022. 5, 7, 8
- [25] Tixiao Shan, Brendan Englot, Drew Meyers, Wei Wang, Carlo Ratti, and Daniela Rus. Lio-sam: Tightly-coupled lidar inertial odometry via smoothing and mapping. In *2020 IEEE/RSJ international conference on intelligent robots and systems (IROS)*, pages 5135–5142. IEEE, 2020. 1
- [26] Claude E Shannon. A mathematical theory of communication. *The Bell system technical journal*, 27(3):379–423, 1948. 8
- [27] Jake Snell, Kevin Swersky, and Richard Zemel. Prototypical networks for few-shot learning. *Advances in neural information processing systems*, 30, 2017. 2
- [28] Youcheng Song, Zhengxing Sun, Qian Li, Yunjie Wu, Yunhan Sun, and Shoutong Luo. Learning indoor point cloud semantic segmentation from image-level labels. *The Visual Computer*, 38(9-10):3253–3265, 2022. 2
- [29] Hugues Thomas, Charles R Qi, Jean-Emmanuel Deschaud, Beatriz Marcotegui, François Goulette, and Leonidas J Guibas. Kpconv: Flexible and deformable convolution for point clouds. In *Proceedings of the IEEE/CVF international conference on computer vision*, pages 6411–6420, 2019. 6
- [30] Jiacheng Wei, Guosheng Lin, Kim-Hui Yap, Tzu-Yi Hung, and Lihua Xie. Multi-path region mining for weakly supervised 3d semantic segmentation on point clouds. In *Proceedings of the IEEE/CVF conference on computer vision and pattern recognition*, pages 4384–4393, 2020. 2
- [31] Yushuang Wu, Zizheng Yan, Shengcai Cai, Guanbin Li, Xiaoguang Han, and Shuguang Cui. Pointmatch: A consistency training framework for weakly supervised semantic segmentation of 3d point clouds. *Computers & Graphics*, 116:427–436, 2023. 2, 6
- [32] Zhonghua Wu, Yicheng Wu, Guosheng Lin, Jianfei Cai, and Chen Qian. Dual adaptive transformations for weakly supervised point cloud segmentation. In *Computer Vision—ECCV 2022: 17th European Conference, Tel Aviv, Israel, October 23–27, 2022, Proceedings, Part XXXI*, pages 78–96. Springer, 2022. 2, 6
- [33] Saining Xie, Jiatao Gu, Demi Guo, Charles R Qi, Leonidas Guibas, and Or Litany. Pointcontrast: Unsupervised pre-training for 3d point cloud understanding. In *Computer Vision—ECCV 2020: 16th European Conference, Glasgow, UK, August 23–28, 2020, Proceedings, Part III 16*, pages 574–591. Springer, 2020. 3
- [34] Xun Xu and Gim Hee Lee. Weakly supervised semantic point cloud segmentation: Towards 10x fewer labels. In *Proceedings of the IEEE/CVF conference on computer vision and pattern recognition*, pages 13706–13715, 2020. 1, 2, 5
- [35] Cheng-Kun Yang, Ji-Jia Wu, Kai-Syun Chen, Yung-Yu Chuang, and Yen-Yu Lin. An mil-derived transformer for weakly supervised point cloud segmentation. In *Proceedings of the IEEE/CVF Conference on Computer Vision and Pattern Recognition*, pages 11830–11839, 2022. 2, 3, 6
- [36] Baochen Yao, Hui Xiao, Jiayan Zhuang, and Chengbin Peng. Weakly supervised learning for point cloud semantic segmentation with dual teacher. *IEEE Robotics and Automation Letters*, 2023. 6, 8
- [37] Yachao Zhang, Zonghao Li, Yuan Xie, Yanyun Qu, Cuihua Li, and Tao Mei. Weakly supervised semantic segmentation for large-scale point cloud. In *Proceedings of the AAAI Conference on Artificial Intelligence*, pages 3421–3429, 2021. 2, 6
- [38] Yachao Zhang, Yanyun Qu, Yuan Xie, Zonghao Li, Shanshan Zheng, and Cuihua Li. Perturbed self-distillation: Weakly supervised large-scale point cloud semantic segmentation. In *Proceedings of the IEEE/CVF International Conference on Computer Vision*, pages 15520–15528, 2021. 2, 6
- [39] Bolei Zhou, Aditya Khosla, Agata Lapedriza, Aude Oliva, and Antonio Torralba. Learning deep features for discriminative localization. In *Proceedings of the IEEE conference on computer vision and pattern recognition*, pages 2921–2929, 2016. 2